Optimal Nanogrid Planning at Building Level

Salar Moradi[a], Vahid Vahidinasab[b], Gaetano Zizzo[a]

[a]*Engineering Department, University of Palermo, Palermo, Italy*
[b]*Engineering Department, Nottingham Trent University, Nottingham, United Kingdom*

Abstract

This paper presents a planning framework for active buildings as an Energy Nano-Grid (ENG), determining the optimal size and generation mix of distributed energy resources (DERs) and battery energy storage (BES) system, the type of ENG that can be either AC or DC, and the optimal energy management (EM). Due to the increasing penetration of battery energy storage devices, electric vehicles (EVs) and even DC loads on the utility side, DC ENGs would potentially be more useful than AC ENGs by reducing the number of converters, facilitating the connection of various types of distributed energy resources and loads to the common bus with simplified interfaces, and mitigating the losses associated with AC/DC energy conversion. Therefore, the selection of the type of ENG is an economic issue where the planning objective includes the investment, operation and maintenance costs of energy resources, the investment costs of battery energy storage (BES) and converters, and the costs/revenues for buying/selling energy from/to the upstream grid or neighbor ENGs. In this way, the proposed program achieves an optimal load sharing. Optimal results might be affected in terms of some system specifications such as the ratio of DC load (from 0.4 to 1) at ENG, the maximum permissible installation capacity of BESs (from 200 to 800 kWh), and maximum discharge power that EVs can deliver to the ENG or upstream network (from 50 to 200 kW). Using some numerical case studies associated with three residential ENGs, result show that increase in the rate of DC load has the highest effect on the type of ENG (DC feeder is adopted for DC load rate 0.6 at ENG 1 and ENG 2, and 0.8 at the third one) through decrease in investment and operation costs, meanwhile, the capacity of BES directly affect the size of generation units, and the maximum discharging power of EVs just support peak load supply due to being out of the park lot during the day. The proposed planning model is analyzed in detail to demonstrate its applicability, effectiveness and control.

Keywords: energy nano-grid; AC/DC hybrid nanogrid; optimal load sharing; PV/wind system; battery energy storage (BES); electrical vehicle (EV); energy management.

1. INTRODUCTION

NOMENCLATURE

The symbols used in this paper are listed and defined in this section.

Indices and Sets	
n	Index for ENGs
t	Index for time interval
d	Index for days in a year
y	Index for years of planning horizon
i	Index for DERs
T_{in}	Set of hours that EVs are at ENG
T_{out}	Set of hours that EVs are out of ENG
Parameters	
NE	Total number of ENGs
NT	Total number of periods [hour]
ND	Total number of days in a year [day]
NY	Total number of years [year]
NI	Total number of DERs at each ENG

CR	Investment cost of DERs [$/kW]
CS	Investment cost of BES [$/kWh]
CRE	Investment cost of rectifiers [$/kW]
CC	Investment cost of converters [$/kW]
CI	Investment cost of inverters [$/kW]
CB	Investment cost of bidirectional converter [$/kW]
CT	Investment cost of transformers [$/kW]
l	Rate of DC load to total load at ENG [%]
L^{max}	Load peak at ENG [kW]
L	Power demand at ENGs [kW]
α	Critical load rate at ENG [%]
P_g^{max}/P_g^{min}	Maximum and minimum power purchased from the grid [kW]
P_s^{max}/P_s^{min}	Maximum and minimum power sold to the grid [kW]
C^p/C^s	Price of power purchased/sold from/to the grid [$]
B	Large positive constant
M^w/M^p	Maintenance cost of wind and photovoltaic generation systems per unit [$/kW]
Q	Efficiency of converters [%]
β	Efficiency of generation for DERs [%]
γ	Coefficient of sunlight intensity for PV systems [%]
$P_{ch}^{max}/P_{dis}^{max}$	Upper limit for charging/discharging power at BES [kW]
$P_{ch}^{min}/P_{dis}^{min}$	Lower limit for charging/discharging power at BES [kW]
$P_{ch,ev}^{max}$	Upper limit for charging power at EV's park lot [kW]
$P_{dis,ev}^{max}$	Upper limit for discharging power at EV's park lot [kW]
$P_{ch,ev}^{min}$	Lower limit for charging power at EV's park lot [kW]
$P_{dis,ev}^{min}$	Lower limit for discharging power at EV's park lot [kW]
$P_{ev,out}^{dis}$	Discharging power per Km for EVs' journey [kW]
$U_s(0)$	Initial available energy at BES [kWh]
$U_{ev}(0)$	Initial available energy at EV's park lot [kWh]
$\Delta U_s/\Delta U_{ev}$	Small off-set energy to avoid end-of-horizon effect at BES and EV park lot [kWh]
P^{max}/P^{min}	Upper and lower limit for the capacity of DERs [kW]
E_s^{max}/E_s^{min}	Upper and lower limit for the capacity of BES [kWh]
$U_{ev}^{max}/U_{ev}^{min}$	Upper and lower limit for energy at EV's park lot [kWh]
N	Total number of EVs at an ENG
D	Average distance of movement each EV traverses a day [Km]
T_l	Time that EVs leave ENG [hr]
λ	Discharge rate of EVs per Km
r	Discount rate
k	Coefficient of net present value
z/Z	Coefficient of upper and lower energy limit for BES
Variables	
IC	Total investment cost [$]
OC	Total operation cost [$]
MC	Total maintenance cost [$]
P	DERs' capacity installed at ENGs [kW]

E	BES capacity installed at ENGs [kWh]
A	Binary variable representing ENG's feeder (0 if ac,1 if dc)
P_g	Power flows from grid to ENGs [kW]
P_c	Power flows from ENGs to the grid [kW]
P_p/P_w	PV and wind power generation at ENG [kW]
P_s^{ch}/P_s^{dis}	Charging/discharging power of BES [kW]
P_{ev}^{ch}/P_{ev}^{dis}	Charging/discharge power of EVs [kW]
I_s^{ch}/I_s^{dis}	Binary variable showing charging/discharging status of BES
I_{ev}^{ch}/I_{ev}^{dis}	Binary variable showing charging/discharging status of EVs
e_s/e_{ev}	Available energy at BES and EVs' park lot [kWh]
e_s^{max}/e_s^{min}	Upper and lower limit for available energy at BES [kWh]
I_g/I_c	Binary variable showing the direction of power exchange between the grid and ENGs
I_R	Binary variable representing the existence of DERs

Symbols and Abbreviations

ENG	Energy Nano-Grid
BES	Battery energy storage
DER	Distributed energy source
EV	Electrical vehicle
EM	Energy management
PV	Photovoltaic

1.1. Aims and Scopes

With the advent of new technologies such as renewable-based micro-energy sources, energy storage systems and small-scale co-generations in the building sector, there is a need for a systemic approach to the planning of building energy systems. The whole systems approach involves evaluating the various components of the system and rethinking the relationships between each of them and even redesigning the system. Confidently, such a complex energy system, faces conflicting challenges of security, equity and sustainability, which are often referred to as the energy trilemma (see Fig. 1). [1-3].

Nowadays, buildings are responsible for about 40% of carbon emissions and any solution to the energy crisis will have to address the issue of energy use in buildings [4]. Recent developments in smart building technologies clearly show that the buildings of the future have the potential to be active and energy self-sufficient entities which, when connected with other active buildings or to the upstream electricity grid, could have the ability to trade energy [5-6].

To enable energy resilient communities that are powered by solar and wind plants and are able to share energy with neighbors and transport systems, this paper proposes a comprehensive techno-economic framework for the optimal planning and load sharing in energy management system (as a tertiary level controller) for the buildings as an Energy Nano-Grids (ENG) that can actively participate in the two-vector energy and transport system.

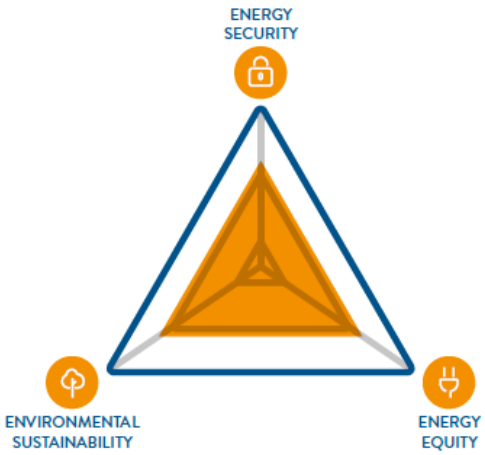

Fig. 1. The energy trilemma triangle [1].

1.2. Research Challenge

The main point of the challenge is to decide on the optimal type of the building-based nanogrid, either AC or DC, based on system specifications such as the DC load ratio at the ENG, the maximum capacity of the installed Battery Energy Storage (BESs) devices and the maximum energy that electric vehicles (EVs) can deliver to the ENG or the upstream network; thus, determining the optimal mix of solar and wind power (S and WP) generators and BESs as generation portfolio.

1.3. Literature Survey

Table 1 presents a taxonomy of existing approaches where previous researches are reviewed and compared. In [7], a networked nanogrid and a battery swapping station (BSS) are considered where nanogrids can share their energy surplus or store it at the BSS to supply power to electric vehicles during peak hours. One of the challenging issues in this study is that energy must be transmitted to the BSS by the delivery system with an increase in the operation and investment costs. The study in [8] presents a planning model for microgrids connected to the upstream grid to measure the optimal size, generation mix of distributed energy resources (DERs) and type of the microgrid. The work evaluates how various factors, such as the entity of the DC and of the critical load and converter efficiency, determine whether microgrids should be DC or AC.

In [9], authors developed the proposed model in [8] and show that in some cases, hybrid AC/DC microgrids can be more economical than other types by reducing the number of converters. In ref. [10], power and voltage control of a hybrid building nanogrid with two AC and DC buses are performed in both grid-connected and off-grid states. In [11], residential units are represented as energy hubs, so, in addition to electrical components, the optimal structural dimensioning of the cogeneration unit, gas boiler and heat storage systems must be considered. Some residential DC nanogrids connected to each other and to the main grid are illustrated in [12]. The import and export of electricity is controlled by an online cyber-physical approach, formulated by Lyapunov optimization. The market-based advantages of nanogrids with photovoltaic energy storage systems are discussed in [13].

In [14], different types of renewable and non-renewable resources like wind turbines, photovoltaic (PV) systems, and fuel cells are taken into consideration in grid-connected nanogrids. In contrast to other studies, the costs of environmental damage from pollutant gases and battery power losses are taken into account in the optimization of the operation management process. A new multi-objective optimization model for energy management in microgrid/nanogrid is proposed in [15] to determine the time of buying or selling electricity to or from the main grid. Ref [16] aims to gain optimal daily power schedule for energy storage systems in microgrids, while the uncertainties associated with load and RESs' available power as well as the time and duration of unscheduled islanding events are considered.

In [17] a robust planning is depicted to determine the optimal expansion of distribution networks with electric vehicle penetration, where the objectives are the expansion/construction of substations and/or charging stations for electric vehicles and the determination of the capacity of renewable resources. The main feature of this study is that the

uncertainty of the load and EV demand, the level of which changes in various time intervals, is modelled through a normal distribution variable, so a scenario-based model such as Monte Carlo simulation is required to solve the program. Ref [18] presents a dynamic programming (DP) technique to optimize load sharing in solar-based DC nanogrids in presence of battery storage. In addition to an optimal load sharing, that paper achieves maximum availability of the solar energy system, minimum fuel consumption and an increase in the battery life cycle.

Kumar .J. et al. have published some recent researches regarding energy management in DC and hybrid microgrids [19-22]. In references [19] and [20], a control based energy management is implemented for a mini and vast DC microgrid respectively, where Maximum Power Point Tracking (MPPT) algorithm is applied to PV system to provide high utilization, and charging/discharging of battery storage system and super capacitors are controlled to respond to dc voltage regulation/load changing and fluctuation, respectively. These works consider only DC nanogrid, where lower control level (usually is called secondary level) is conducted as energy management system, and upper level that includes planning, generations' size and mix are not modeled. However, in [21], authors have proposed a new configuration for DC microgrids in isolated communities like a village, where the system aims to utilize unused stored water to generate electricity through solar pumping units. The same controllers as those in [19, 20] are characterized, and numerical analysis is done for designing the size of water tank, pumps, PV arrays, and small batteries, whereas, economic study has been ignored. Ref. [22], however, provides a more comprehensive approach to determine the most optimized combination of AC and DC mini grids in hilly districts in India, so that minimizes the total costs. The objective function incorporates environmental and reliability-based constraints, and the program is solved using Genetic algorithm.

Table 1. TAXONOMY OF PLANNING AND ENERGY MANAGEMENT OF NANOGRIDS

References	Network level	Planning result			Bus type analysis	BES penetration	EVs penetration	Mathematical modeling
		Energy management	Optimal sizing	Generation mix				
[7]	nanogrid	✓	✓			✓		MILP
[8]	microgrid		✓	✓	✓	✓		MILP
[9]	microgrid		✓	✓	✓	✓		MILP
[10]	nanogrid	✓				✓		
[11]	nanogrid	✓	✓					NLP
[12]	nanogrid	✓						
[13]	nanogrid		✓			✓		LO
[14]	nanogrid	✓				✓		MO
[15]	nanogrid	✓				✓		LP
[16]	microgrid	✓				✓		MILP
[17]	EDS		✓	✓			✓	MILP
[18]	nanogrid	✓				✓		DP
[19]	nanogrid	✓				✓		
[20]	microgrid	✓				✓		
[21]	microgrid	✓	✓			✓		
[22]	nanogrid	✓		✓	✓			GA
This paper	nanogrid	✓	✓	✓	✓	✓	✓	MILP

LO= Lyapunov Optimization MO= Multi-Objective EDS= Electrical Distribution Systems DP= Dynamic Programming GA=Genetic Algorithm

1.4. Contributions

This paper proposes a planning framework for small scale power grids called energy nano-grids (ENGs) including buildings with renewable energy sources. This planning program aims to provide an energy management system in tertiary control level, where the following four problems are characterized and solved through an optimization program: A) determining the optimal energy resources mix, meaning local RESs could be PV system or/and wind turbine, their size, and installed capacity that is needed for BES; B) determining the economically optimal type of the

main feeder for nanogrid (AC or DC), where RESs and flexible sources like BES and EV park lot are connected to the nanogrid; C) to conduct different scenarios correlating different range of the maximum BES's installed capacity, maximum discharge power rate in park lot, and rate of DC load to identify corresponding threshold values making a nanogrid more economically viable solution than the AC one; and D) executing properly and optimally a 24-hour load sharing among RESs, upstream network, flexible sources, and other nanogrids.

To handle and achieve abovementioned issues, the proposed nanogrid planning framework minimizes the total cost, which includes the investment costs of the energy resources and converters, the costs/revenues of energy imported/exported from/to the upstream grid or neighboring nanogrids, and the operating costs of the nanogrids. In short, the main contributions of this paper can be recapitulated as follows:

- Optimal planning and size of the renewable energy resources and energy storage devices;
- Determination of the economically optimal types of the main feeder in nanogrid (AC or DC);
- Determination of the optimal threshold ratios for maximum installation capacity of BESS, maximum discharge power rate of electric vehicles and DC loads rate, by conduction different scenarios, that make a DC nanogrid more affordable option than an AC one;
- Preparing a techno-economic energy management framework.

The remainder of the paper is organized as follows. Section 2 provides outlooks for both AC and DC nanogrids and the proposed planning and problem formulation are modeled, and numerical results of the planning program for different energy scenarios in three ENGs are presented in Section 3. Section 4 analyses and compares the results in deep, and Section 5 concludes the paper.

2. PLANNING FORMULATION

2.1. Mathematical model

Fig. 2 and Fig. 3 show a precise architecture of DC and AC energy nanogrids respectively. At both types of ENGs, each ENG is connected to the upstream network through an AC common bus. In the DC ENG, a bidirectional DC/AC converter is required to connect the AC common bus (the point of common coupling) to the DC bus. The EVs' park lot, the BES and the solar systems are connected to the DC bus through DC/DC converters. In addition, wind turbine and AC loads at the ENG are connected to the DC bus using rectifiers and inverters respectively.

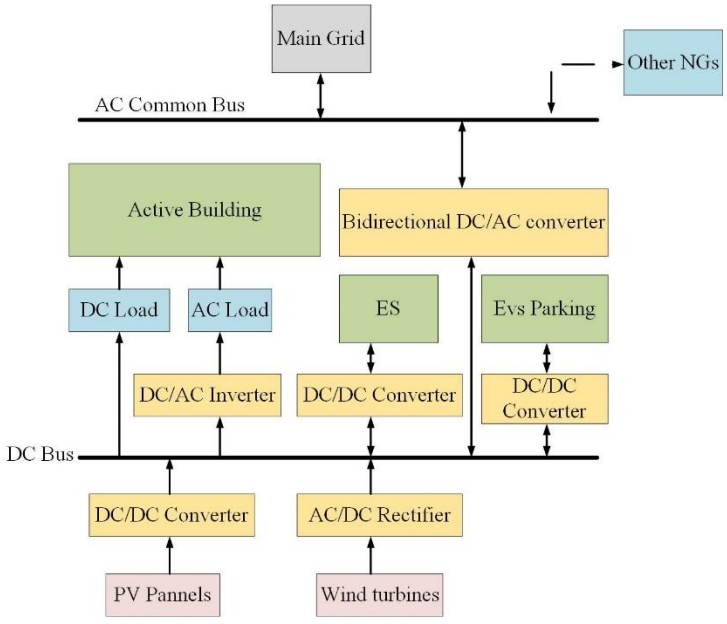

Fig. 2. Architecture of a DC nanogrid

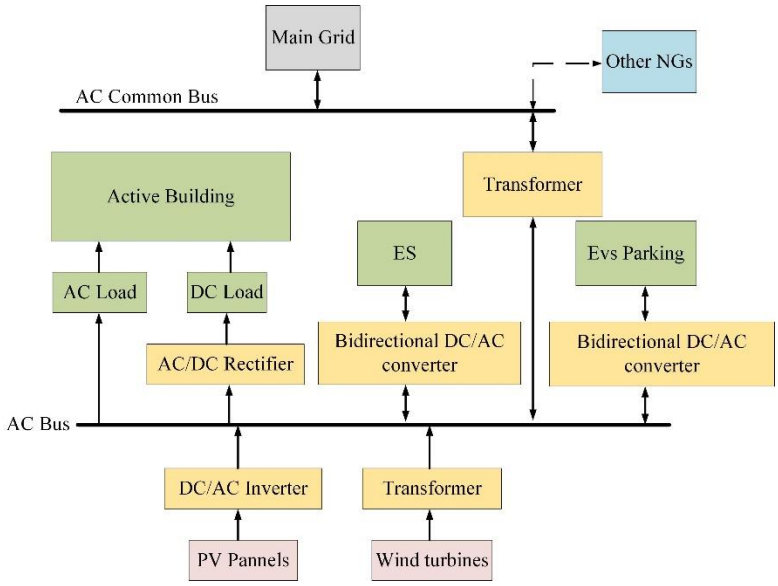

Fig. 3. Architecture of an AC nanogrid

In the AC ENG, the AC common bus and the wind turbine are connected to the internal AC bus by transformers. EVs' park lots and BESs are connected to the AC bus through bidirectional DC/AC converters. Inverters are needed between solar systems and the AC bus, and rectifiers to connect DC loads.

In the proposed planning model, the total cost of ENGs, including investment (IC), operation (OC) and maintenance (MC) costs, must be minimized to achieve an optimal type of ENG, and size and generation mix. Therefore, the objective function of the proposed model is as follows:

$$C_{total} = \sum_{n=1}^{NE} IC(n) + OC(n) + MC(n) \quad (1)$$

In this paper, the maintenance cost is only restricted to the maintenance of DERs and not include the maintenance cost of converters since it has been supposed that all converters are not repairable and they have to be replaced with new ones after their lifetime, which is the same as the planning period horizon. Investment cost includes the capital price of all DERs and converters, and can be written as two equations below based on ENG's type DC or AC.

$$\begin{aligned} &-B(1-A(n)) \le IC(n) - [\sum_{y=1}^{NY} k(y) \sum_{i=1}^{NI} CR(i)P(n,i) + \\ &\sum_{y=1}^{NY} k(y)E(n)CS + \sum_{y=1}^{NY} k(y)P(n,1)CRE + \sum_{y=1}^{NY} k(y)P(n,2) \\ &CC + \sum_{y=1}^{NY} k(y)(1-l(n))L^{\max}(n)CI + \sum_{y=1}^{NY} k(y)P_{ch}^{\max}CC \\ &+ \sum_{y=1}^{NY} k(y)P_{ch,ev}^{\max}CC + \sum_{y=1}^{NY} k(y)P_{g}^{\max}CB] \le B(1-A(n)) \qquad \forall n \end{aligned} \quad (2)$$

$$
\begin{aligned}
&-BA(n) \le IC(n) - [\sum_{y=1}^{NY} k(y) \sum_{y=1}^{NY} \sum_{i=1}^{NI} CR(i) P(n,i) + \\
&\sum_{y=1}^{NY} k(y) E(n) CS + \sum_{y=1}^{NY} k(y) P(n,1) CT + \sum_{y=1}^{NY} k(y) P(n,2) \\
&CI + \sum_{y=1}^{NY} k(y) l(n) L^{\max}(n) CRE + \sum_{y=1}^{NY} k(y) P_{ch}^{\max} CB \\
&+ \sum_{y=1}^{NY} k(y) P_{ch,ev}^{\max} CB + \sum_{y=1}^{NY} k(y) P_{g}^{\max} CT] \le BA(n) \qquad \forall n
\end{aligned} \tag{3}
$$

According to Eq. 2, if planning prefers the DC ENG, variable *A* sets to 1 and (3) would be free; thus, the investment cost is equal to (2). Conversely, if planning chooses the AC ENG, variable *A* is 0 and (2) would be free; in this case, the investment cost would be equal to (3). It is worth mentioning that the DERs set (*i*) includes both wind and photovoltaic power systems: *i*=1 indicates wind and *i*=2 indicates solar. Equations (4) and (5) below represent the operation and maintenance costs, which are the cost of purchasing and selling energy from/to the upstream network, and of the DERs' repair and refurbishment, respectively, and Eq. (6) refers to the coefficient of the net present value.

$$
OC(n) = \sum_{y=1}^{NY} k(y) \sum_{d=1}^{ND} \sum_{t=1}^{NT} C^{p} P_{g}(n,t) - \sum_{y=1}^{NY} k(y) \sum_{d=1}^{ND} \sum_{t=1}^{NT} C^{s} P_{c}(n,t) \qquad \forall n \tag{4}
$$

$$
MC(n) = \sum_{y=1}^{NY} k(y) M^{w} P(n,1) + \sum_{y=1}^{NY} k(y) M^{p} P(n,2) \qquad \forall n \tag{5}
$$

$$
k(y) = 1 / (1+r)^{y-1} \qquad \forall y \tag{6}
$$

Other constraints can be divided into three categories: limits and constraints for the power balance equation and DER generation, constraints for energy trading between ENGs and the upstream grid, and constraints for BESs and EV's park lots.

2.2. Power balance and generation

Equations and inequalities (7)-(12) represent generation-related constraints. Equations (7) and (8) show the hourly power balance for both DC and AC ENGs during a day. Like for the investment cost equations, if planning prefers the DC ENG, variable *A* is 1, and (8) would be free; so the power balance equation would match (7). Conversely, if planning chooses the AC ENG, variable *A* is equal to 0, and (7) gets free. As a result, the power balance formulation would be equal to (8).

$$
\begin{aligned}
&-B(1-A(n)) \le Q[P_{p}(n,t) + P_{w}(n,t) + P_{g}(n,t) + P_{s}^{dis}(n,t) \\
&+ P_{ev}^{dis}(n,t)] - Q[P_{s}^{ch}(n,t) + P_{ev}^{ch}(n,t)] - l(n) L(n,t) - \\
&(1-l(n)) L(n,t)/Q - P_{c}(n,t)/Q \le B(1-A(n)) \qquad \forall n,t
\end{aligned} \tag{7}
$$

$$
\begin{aligned}
&-BA(n) \le Q[P_{p}(n,t) + P_{s}^{dis}(n,t) + P_{ev}^{dis}(n,t)] \\
&+ P_{w}(n,t) + P_{g}(n,t) - Q[P_{s}^{ch}(n,t) + P_{ev}^{ch}(n,t)] - \\
&l(n) L(n,t)/Q - (1-l(n)) L(n,t) - P_{c}(n,t) \le BA(n) \qquad \forall n,t
\end{aligned} \tag{8}
$$

Inequality (9) states that DERs in each ENG must be able to supply, at any time, at least a predefined critical load (α is the percentage of critical load on the maximum load).

Equations (10) and (11) represent the output power limit for DERs, where β is the efficiency of generation for DERs and γ is a coefficient less and equal than 1 giving sunlight intensity during the day (0 in the absence of sun and 1 at noon). Equation (12) expresses the upper and lower limits for the installed capacity of DERs, and (13) shows that it is obligatory for an ENG to have at least one kind of DERs in the problem formulation.

$$\sum_{i=1}^{NI} P(n,i) \geq \alpha L^{\max}(n) \qquad \forall n \tag{9}$$

$$P_w(n,t) \leq \beta P(n,1) \qquad \forall n,t \tag{10}$$

$$P_p(n,t) \leq \beta\gamma(t) P(n,2) \qquad \forall n,t \tag{11}$$

$$I_R(n,i) P^{\min}(n,i) \leq P(n,i) \leq I_R(n,i) P^{\max}(n,i) \qquad \forall n,i \tag{12}$$

$$\sum_{i=1}^{NI} I_R(n,i) \geq 1 \qquad \forall n \tag{13}$$

Since this paper implements an energy management system in tertiary level (optimal load sharing), lower control levels (secondary and primary) are not discussed, assuming they are done well through converters' controller. The note is that, the capacity (size) of DERs, that are going to be installed, is a variable calculated in the planning process. Then, these power set points are delivered to local controller of the converters. To PV system, this paper conducts a Constant Power Generation (CPG) control scheme presented in [23, 24], where the PV output voltage is continuously perturbed away from the maximum power point in the CPG operation mode in order to match the PV output power according to the set point. Therefore, Eq. (11) is characterized to represent this concept. In this equation, parameter $\boldsymbol{\gamma}$ indicates maximum generation of PV system in per unit (p.u.) (in association with irradiance and temperature) that is multiplied to the size of the PV to calculate the maximum output power for each hour. To wind system, a blade pitch control is considered to generate constant power. Readers may refer to Ref. [25] to understand more blade pitch control. For both PV and wind systems, if the program choose maximum power, controllers follow Maximum Power Point Tracking (MPPT) mode; and, inversely, for power references below than maximum value, they conduct constant power generation mode.

2.3. Energy Trading Constraints

Inequalities (14) and (15) restrict power trading between ENG and upstream network to their bounds, and (16) represents that to sell and purchase energy to/from the grid may not be happened simultaneously.

$$I_g(n,t) P_g^{\min} \leq P_g(n,t) \leq I_g(n,t) P_g^{\max} \qquad \forall n,t \tag{14}$$

$$I_c(n,t) P_s^{\min} \leq P_c(n,t) \leq I_c(n,t) P_s^{\max} \qquad \forall n,t \tag{15}$$

$$I_g(n,t) + I_c(n,t) \leq 1 \qquad \forall n,t \tag{16}$$

2.4. BES and EV constraints

Constraints (17)-(26) express BES's limits. Inequalities (17)-(19) represent that installed capacity, charging/discharging power rates of the BES must not exceed their technical bounds, while (20) implies that batteries must not be charged and discharged at the same time.

$$E_s^{\min} \leq E(n) \leq E_s^{\max} \qquad \forall n \tag{17}$$

$$I_s^{ch}(n,t)P_{ch}^{\min} \le P_s^{ch}(n,t) \le I_s^{ch}(n,t)P_{ch}^{\max} \qquad \forall n,t \tag{18}$$

$$I_s^{dis}(n,t)P_{dis}^{\min} \le P_s^{dis}(n,t) \le I_s^{dis}(n,t)P_{dis}^{\max} \qquad \forall n,t \tag{19}$$

$$I_s^{ch}(n,t) + I_s^{dis}(n,t) \le 1 \qquad \forall n,t \tag{20}$$

Equations (21) and (22) show the hourly available energy at the storage system, while (23)-(25) restrict this energy to its upper and lower limits. Inequality (26) tries to prevent the energy of the last hour at BES from not being much more or lower than that of the first hour.

$$e_s(n,t) = e_s(n,t-1) + P_s^{ch}(n,t)Q - P_s^{dis}(n,t)/Q \qquad \forall n, t > 1 \tag{21}$$

$$e_s(n,t) = U_s(0) + P_s^{ch}(n,t)Q - P_s^{dis}(n,t)/Q \qquad \forall n, t < 2 \tag{22}$$

$$e_s^{\min}(n) \le e_s(n,t) \le e_s^{\max}(n) \qquad \forall n,t \tag{23}$$

$$e_s^{\min}(n) = zE(n) \qquad \forall n \tag{24}$$

$$e_s^{\max}(n) = ZE(n) \qquad \forall n \tag{25}$$

$$U_s(0) - \Delta U_s \le e_s(n,t) \le U_s(0) + \Delta U_s \qquad \forall n, t > 23 \tag{26}$$

The rest of the inequalities refer to EVs in which (27)-(33) have approximately the same definition as those for BES because EVs can be operated like battery storage system. Equations (34) and (35) point that when EVs are out of the ENG's park lot, they can not be charged or discharged. Finally, equation (36) explains that EVs have to be charged with a minimum energy level needed for daily journey.

$$I_{ev}^{ch}(n,t)P_{ch,ev}^{\min} \le P_{ev}^{ch}(n,t) \le I_{ev}^{ch}(n,t)P_{ch,ev}^{\max} \qquad \forall n, t \in T_{in} \tag{27}$$

$$I_{ev}^{dis}(n,t)P_{dis,ev}^{\min} \le P_{ev}^{dis}(n,t) \le I_{ev}^{dis}(n,t)P_{dis,ev}^{\max} \qquad \forall n, t \in T_{in} \tag{28}$$

$$I_{ev}^{ch}(n,t) + I_{ev}^{dis}(n,t) \le 1 \qquad \forall n,t \tag{29}$$

$$e_{ev}(n,t) = e_{ev}(n,t-1) + P_{ev}^{ch}(n,t)Q - P_{ev}^{dis}(n,t)/Q - P_{ev,out}^{dis}(n,t) \qquad \forall n, t > 1 \tag{30}$$

$$e_{ev}(n,t) = U_{ev}(0) + P_{ev}^{ch}(n,t)Q - P_{ev}^{dis}(n,t)/Q - P_{ev,out}^{dis}(n,t) \qquad \forall n, t < 2 \tag{31}$$

$$U_{ev}^{\min} \le e_{ev}(n,t) \le U_{ev}^{\max} \qquad \forall n,t \tag{32}$$

$$U_{ev}(0) - \Delta U_{ev} \le e_{ev}(n,t) \le U_{ev}(0) + \Delta U_{ev} \qquad \forall n, t > 23 \tag{33}$$

$$P_{ev}^{ch}(n,t) = 0 \qquad \forall n, t \in T_{out} \;\; P_{ev}^{ch}(n,t) = 0 \qquad \forall n, t \in T_{out} \tag{34}$$

$$P_{ev}^{dis}(n,t) = 0 \qquad \forall n, t \in T_{out} \tag{35}$$

$$e_{ev}(n,T_l) \geq N\lambda D(n) \qquad \forall n \tag{36}$$

In this paper a mixed-integer linear programming (MILP) formulation is considered to solve the optimal planning for residential energy nanogrids including DERs' and BES's mix and size, determining the type of ENGs (DC or AC) and the 24-hourly optimal load sharing under different situations and scenarios. The program is solve using Cplex solver in GAMS tool.

3. CASE STUDY

To illustrate the performance and benefits of the proposed planning model, three residential buildings are considered as three ENGs which are connected to the upstream network through an AC bus (see Fig. 2 or Fig.3). Each ENG is a residential tower with a park lot for hybrid electric vehicles which is able to charge and discharge vehicles' battery. In addition, there are 100 units at each ENG, and it is assumed that all units have an EV. The ENGs are supposedly located in Australia and the load data has been extracted from 300 residential customers there **[26]**. Fig. 4 displays the hourly load demand of the three ENGs under study.

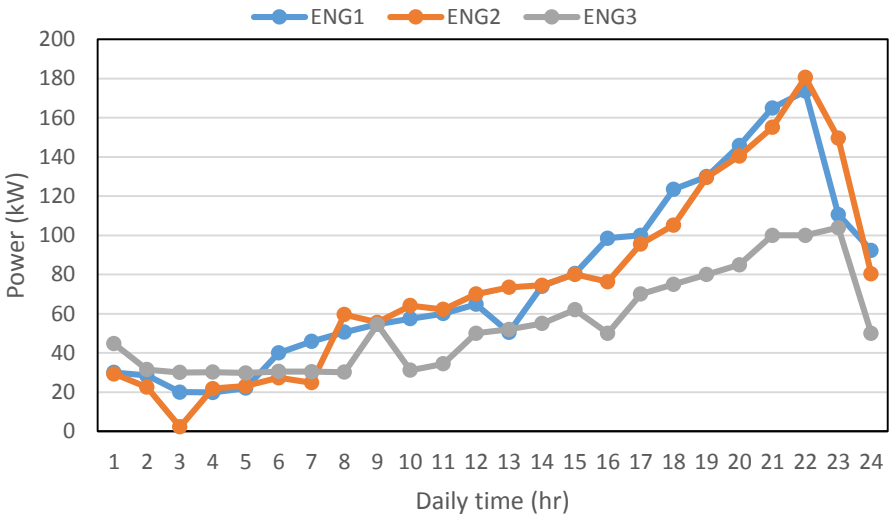

Fig. 4. Hourly power demand of the three residential ENGs

Mitsubishi SUV (6 charge hour, 240 V, 10 A, 54 Km, 12 kWh) as one of the popular Plug-in Hybrid Electrical Vehicles (PHEVs) is selected for this study [27]. Data related to the average daily journey in Australia is found in [28]. Planning horizon, discount rate, coefficient of upper and lower energy limit for BES, and the time at which EVs leave the ENGs are 10 years, 0.1, 0.1, 0.9, and 6:00 AM, respectively. EVs are supposed to go back park lot at 8:00 PM, so their batteries might be charged and discharged before 6 AM. Investment and maintenance cost of DERs and BESs, and investment cost of converters have been drawn from [29], [30], [31], and [32]. The cost-related characteristics of DERs and converters are provided in Table 2.

Table 2. CHARACTERISTICS OF CONVERTERS AND DERS

Converters, BES, and DERs	Investment cost ($/kW(h))	Maintenance cost ($/kW)
Inverter	58	-
Rectifier	40	-
DC/DC converter	65	-
Bidirectional DC/AC	80	-
Transformer	30	-
BES	100	-
Wind turbine	2800	30
PV system	2000	20

As it was said before, the main goal of this paper is to evaluate how some parameters may change the type of ENG, the mix of generation, and the optimal planning and operation of ENGs. In this study, these parameters are the rate of DC load at the ENGs, changes in the maximum permissible capacity of BES, and the maximum discharge power rate of EVs. Therefore, as follows, four cases are projected to assess these aims.

Note that, the initial available energy (state of charge) inside BES at the first hour before starting the programming depends on the scenarios are defined in the following subsections, but in general, for BES system, it is about 80% of the capacity. For example, in a case that battery capacity is fixed (800 kWh), initial energy value is 650 kWh. For electrical vehicles' battery, however, this rate is 50% of the corresponding capacity.

3.1. Case Base

This is the first case of programming. In this case, the rate of DC load for all three ENGs is 0.5, the upper bound for permissible installation capacity of BES is set on the highest value (800 kWh), and the maximum discharge power rate of EVs to support demand supply is considered equal to its peak that is 200 kW. The results of the planning for this case are represented in Table 3.

Table 3. PLANNING RESULTS OF THE CASE BASE.

ENGs	A	PV installed capacity (kW)	Wind installed capacity (kW)	BES installed capacity (kWh)	Investment cost ($)	Operation cost ($)	Maintenance cost ($)
ENG 1	0	145.5	0	774	3040706.1	9364.4	23715.8
ENG 2	0	100	0	774	2910217	18792.7	22322.5
ENG 3	0	0	100	774	2185093.76	416083	13518

3.2. Case 1

In this case, the effect of changes in the rate of DC load at three ENGs on the type of nanogrid, DERs' mix and capacity, investment and operation costs and daily load sharing are evaluated. The parameter α increases from 0.4 to 1 by 0.2 steps. Other parameters are fixed at their base values as those in the case base. The results of the planning in case 1 are shown in Table 4.

Table 4. PLANNING RESULTS OF CASE 1.

α	ENGs	A	PV installed capacity (kW)	Wind installed capacity (kW)	BES installed capacity (kWh)	Investment cost ($)	Operation cost ($)	Maintenance cost ($)
0.4	ENG 1	0	116.9	0	774	3035341.4	37745.7	23708.7
	ENG 2	0	110	0	774	2712376	26028.1	20277
	ENG 3	0	0	100	774	2182284.7	410684.1	13518
0.6	ENG 1	1	123.4	0	774	3136466.9	39280.4	25033.4
	ENG 2	1	100.8	0	774	2699869.2	128717.4	20438.8
	ENG 3	0	0	100	774	2187902.8	421481.9	13518
0.8	ENG 1	1	120	0	774	3057498.4	49184	24343
	ENG 2	1	100	0	774	2670392.7	97749.3	20277
	ENG 3	1	0	100	774	2170622.9	444151.3	13518
1	ENG 1	1	118.1	0	774	3006967.9	14731.4	23953
	ENG 2	1	100	0	774	2656232.8	86900.1	20277
	ENG 3	1	0	100	774	2162476.7	432238.7	13518

3.3. Case 2

This case analysis how an increase in the upper bound for allowable installation capacity of BES can change the type of ENG, the mix and capacity of generation and investment and operation costs, and the way that electrical energy flows as well. This parameter E_s^{max} rises from 200 to 800 kWh by 200 kWh steps. The rate of DC load and peak of EVs' discharge power are put on their basic amount (0.5, 200 kW). Table 5 shows the planning consequences of this case.

3.4. Case 3

This case evaluates how increase in the maximum discharge power rate of electric vehicles might change the type of ENG, the mix and size of generation units, investment and operation costs, and the 24-hour load sharing. It is obvious that EVs may not supply ENGs demand power with their maximum discharge power rate because of being out of park

lot and unexpected events. This type of flexible resources' behavior is largely unpredictable. So, this paper considers changes in the availability amount of this parameter ($P_{dis,ev}^{max}$) rather than stochastic approaches. This parameter $P_{dis,ev}^{max}$ rises from 50 to 200 kW with 50 kW steps. The rate of DC load and upper bound for installation capacity of BES are fixed on their basic values (0.5 and 800 kWh). Table 6 illustrates the planning results for this case.

Table 5. PLANNING RESULTS OF CASE 2.

E_s^{max}(KWh)	ENGs	A	PV installed capacity (kW)	Wind installed capacity (kW)	BES installed capacity (kWh)	Investment cost ($)	Operation cost ($)	Maintenance cost ($)
200	ENG 1	0	145.5	0	190.1	3191888.6	-130717.6	29502.5
	ENG 2	0	100	0	190.1	2322565.1	50415.2	20277
	ENG 3	0	0	100	190.1	1790400.1	425971.7	13518
400	ENG 1	0	101.1	0	390	2479171.3	94515.8	20514.2
	ENG 2	0	100	0	390	2457745.6	27575.6	20277
	ENG 3	0	0	100	390	1925580.6	413256.4	13518
600	ENG 1	1	123.4	0	579	3011429.7	25698	25033.4
	ENG 2	0	110	0	579	2585416	24473.2	20277
	ENG 3	0	0	100	579	2053251	409859.3	13518
800	ENG 1	0	116.9	0	774	3040706.1	9364.4	23715.8
	ENG 2	0	110	0	774	2910217	18792.7	22322.5
	ENG 3	0	0	100	774	2185093.7	416083	13518

Table 6. PLANNING RESULTS OF CASE 3.

$P_{dis,ev}^{max}$	ENGs	A	PV installed capacity (kW)	Wind installed capacity (kW)	BES installed capacity (kWh)	Investment cost ($)	Operation cost ($)	Maintenance cost ($)
50	ENG 1	0	117.8	0	774	3058044.3	10856	23899.6
	ENG 2	0	100	0	774	2717258.7	37494.9	20277
	ENG 3	0	0	100	774	2185093.7	416083	13518
100	ENG 1	0	119.1	0	774	3083212.8	33947.2	24166.4
	ENG 2	0	100	0	774	2717258.7	30403.8	20277
	ENG 3	0	0	100	774	2185093.7	416083	13518
150	ENG 1	0	17.8	0	774	3058044.3	7099.6	23899.6
	ENG 2	0	111.2	0	774	2932775.4	-7633.9	22561.7
	ENG 3	0	0	100	774	2185093.7	416083	13518
200	ENG 1	0	116.95	0	774	3040706.1	9364.4	23715.8
	ENG 2	0	110	0	774	2910217	18792.7	22322.5
	ENG 3	0	0	100	774	2185093.7	416083	13518

4. DISCUSSION

Starting from the case base, as it can be seen from Table 3, it is noticeable that the program would choose AC type for all three ENGs ($A = 0$) because, in this common occasion, the cost of all converters in the DC ENGs is significantly higher than that of an AC one. Customers are supplied by photovoltaic plants at the first two ENGs and by wind plants at the third ENG. Since the installed capacity of PV systems at ENG1 and ENG2 are larger than wind system at ENG3, investment and maintenance costs of ENG1 and ENG2 are higher than those at ENG3.

Looking at both Table 3 and Fig. 5, simultaneously, although solar systems can not generate energy in the absence of sun (night hours) and the peak load at these ENGs (ENG 1 and ENG 2) is higher than peak load at ENG3, program would prefer to install photovoltaic plants for both ENG1 and ENG2. There are two reasons: first, the investment cost of the solar system is lower than that of the wind one, and second, they can sell electrical energy to the upstream network at noon which leads to a considerable decrease in the operation cost. To reach a balance between operation and investment cost, the program would rather set lower wind power generation than peak load at ENG3. In this case ENG's load is provided at peak hours through purchasing energy from the upstream grid. Therefore, operation cost at this nanogrid has a meaningful value.

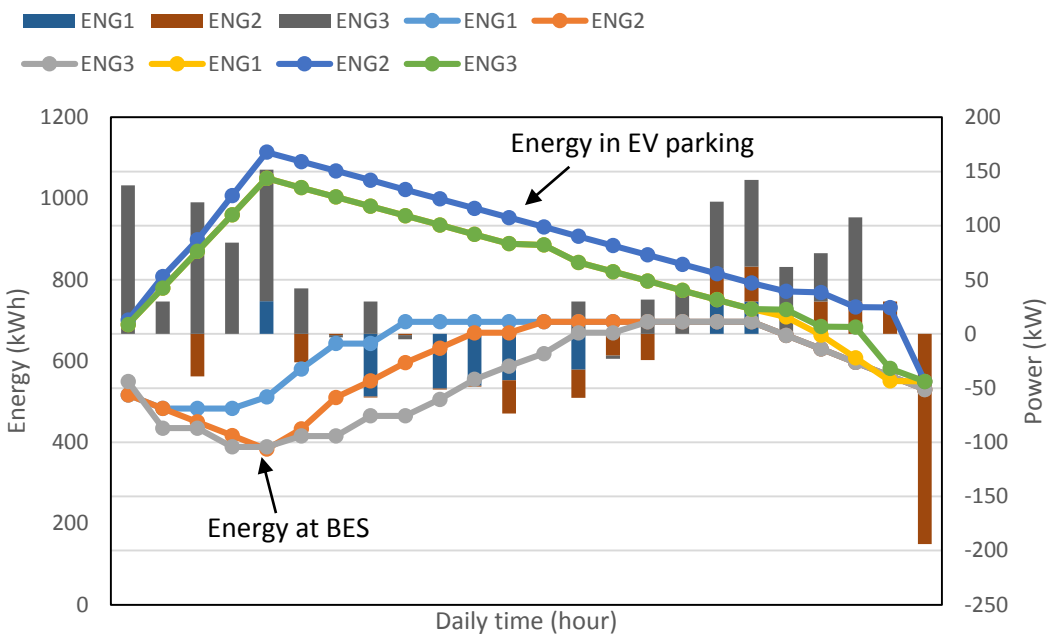

Fig. 5. Daily energy and power trading in the case base.

Fig. 5 shows the daily energy available at the BES system and EVs parking (line graphs) and the daily power trading (bar charts) in the case base. It is worth saying, due to this fact that all ENGs are residential buildings with similar power demand behavior, these variables at each building would change as other. It can be derived that electrical vehicles in park lot, unlike batteries at BES system, are charged at early hours of a day. This is reasonable because EVs should be prepared to go out till 20 PM. after that they can share their energy to supply load and/or trade with the main grid. Conversely, the BES system is discharged at the first hours to help supply ENGs' load demand, then it is charged to peak hours, largely by PV systems for ENG1 and ENG2 and by purchasing energy from the main grid for ENG3. Finally, it has the same trend as EVs during peak hours. Figure 5 represents the reason why operation cost at ENG3 is significantly more than other ones. It mostly receives electrical energy from the upstream network during a day which causes to drop in DER's investment cost.

Looking at Table 4, some conclusions can be drawn. First, as expected, a change in the rate of DC load affects the type of ENGs. An increase in the rate of DC load, according to investment cost equation for DC ENG (Eq. 2), results in a decrease in the term related to the inverter in this equation, and in the case $l(n) = 1$, where there is no AC load, it would be deleted. Conversely, according to (3), the investment cost for rectifier rises when l increases. So, investment cost in DC case would be much lower than that in AC one. Power balance equations can also make this analysis clearer. In fact, as l increases, considering converters efficiency, DC ENG needs less energy from the upstream grid and/or other sources to supply customers than AC ENG. Therefore, DC ENG would be preferable to AC one. Since the peak load at ENG1 and ENG2 is higher than at ENG3, less increase in l at the first two ENGs leads to a more considerable reduction in the investment cost. So, the optimal threshold ratios of l is 0.6 for ENG 1 and ENG2 and 0.8 for ENG3.

Moreover, due to not change in load demand and upper bound of capacities, the mix generation and installed capacity of DERs and BES have not been updated. So, investment and maintenance costs have not approximately changed, and the little fluctuations in Table 4 are due to an increase in l; therefore, non-meaningful changes in investment cost of rectifiers and inverters is carried out.

Another point that emerges from the examination of Table 4 concerns the operating cost. There is a sharp increase in the operating cost of ENG2 with an increase of l from 0.4 to 0.6. There is an acceptable reason for this, namely that by changing the type of ENG and considering the power balance equation in the DC state (see (7)), the efficiency of the converters causes the ENG to purchase more energy from the upstream grid. Furthermore, since the sale and purchase of energy from/to the upstream grid may not occur simultaneously, the operating cost would increase (see (4)). The same assessment is valid for an increase in operation cost at ENG1, while due to higher peak load than ENG2, it rises when l goes up excepting when $l(n) = 1$, where AC load term in power balance equation, which is

connected to converter in DC power balance equation (see (7)) would be disappeared, so there would be less need to purchase energy. Nevertheless, its noticeable drop once *l* rises from 0.8 to 1 is for the term of AC load.

This point could be clearer from the bar chart Fig. 6 showing trading energy between ENGs and the main grid. It could be said that, although the output of wind plants is not restricted by environmental parameters like irradiance for photovoltaic systems, ENG3 would almost buy energy whole a day from the main grid; the convincing reason is expensive investment cost for this system. According to the line graph in Fig. 6, it is expected that a change in the DC load rate will not lead to any significant change in the energy stored by the BES and EV parking, because they are largely limited by their local parameters.

In case 2, looking at Table 5, the impact of increase in the upper bound of the installed capacity of BES has been assessed. It is projected that a rise in E_s^{max} may not make a considerable difference in the type of ENGs since both DC and AC investment cost equations (see (2) and (3)) have the term related to BES's investment cost in common. Once $E_s^{max} = 600$ kWh, the type of ENG1 is DC which is caused by a change in the pattern of BES's charge and discharge so that it can decrease operation cost when DC ENG is chosen.

Another predictable point is that once $E_s^{max} = 200$ kWh, ENG1 ,where there is a higher peak load than other ones, must use a solar power system with more capacity; this leads to a surge in investment costs in this ENG. Note that the capacity of the solar system rises so much, meaning the amount of electrical energy which the ENG sells to the upstream network is more than that of ENG purchases from it; therefore, the operation cost at this ENG is negative. It can be seen that, the more amount for E_s^{max}, the more available energy for selling, and the less need to buy energy from the upstream grid. So, operation costs would decrease. While, for ENG2 and ENG3, a change in E_s^{max}, according to Table 5, might not make any sensible changes in the installation capacity of DERs. As a result, maintenance costs at these ENGs remain stable. When this parameter increases, investment cost at these two ENGs rises due to an increase in the cost of BES, whereas their operation cost dips because of more energy sold and less energy purchased.

From the line graph in Fig. 7, it is obvious that higher E_s^{max} availability has caused more installation capacity of the BES system. Another noteworthy point is that an increase in hourly energy available at the electric vehicle park lots, due to the increase in the amount of energy at the BES, allows them to share their batteries to supply energy to the load or sell it to the main grid; therefore, the ENGs, especially ENG3 due to its lower peak load than the others, do not need the electric vehicles to supply energy. The bar chart in Fig. 7 advocates the evaluation above for case 2. ENG1 with bigger installation capacity sells considerable energy to the main grid. When $E_s^{max} = 400$ kWh, it has a wild drop, making ENG1 not trade energy with the upstream network. $E_s^{max} = 600$ kWh leads to higher capacity of the solar system, and to more balance trading. Considering both bar chart and Table 5, because the generation capacity at ENG3 is low and constant, more capacity of BES system does not considerably change energy trading pattern but increases the investment cost.

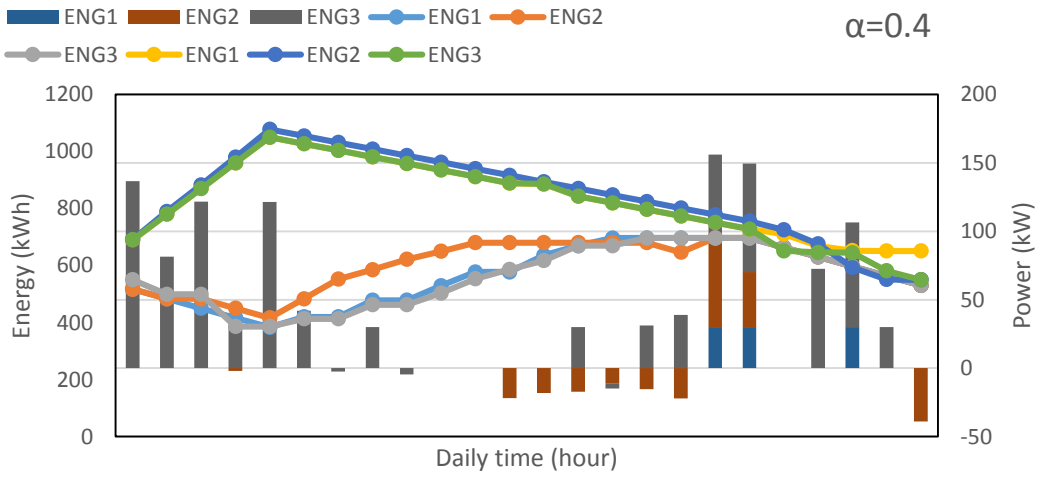

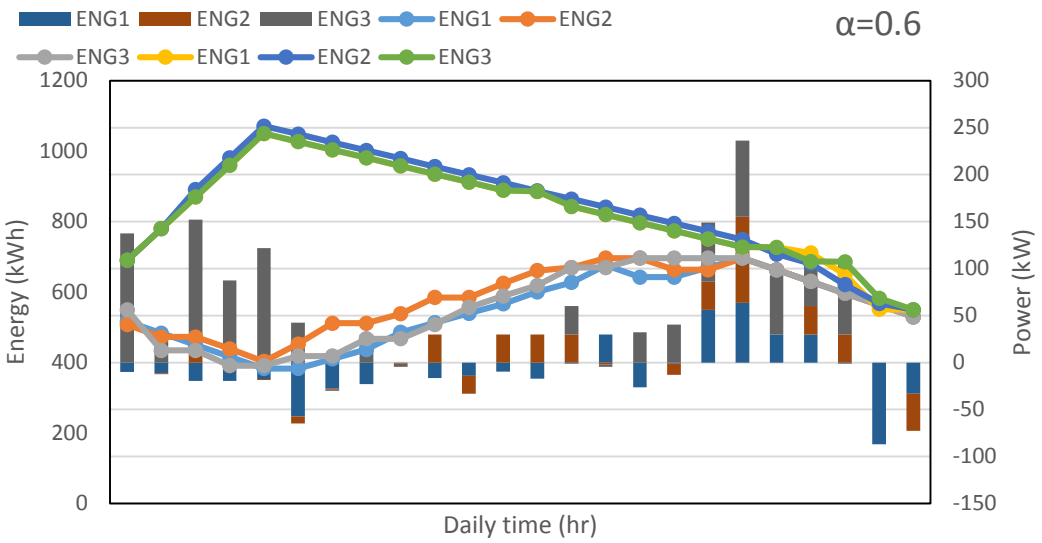
ENG1
ENG2
ENG3
ENG1
ENG2
ENG3
ENG1
ENG2
ENG3
α=0.6
Energy (kWh)
Power (kW)
Daily time (hr)
0
200
400
600
800
1000
1200
-150
-100
-50
0
50
100
150
200
250
300

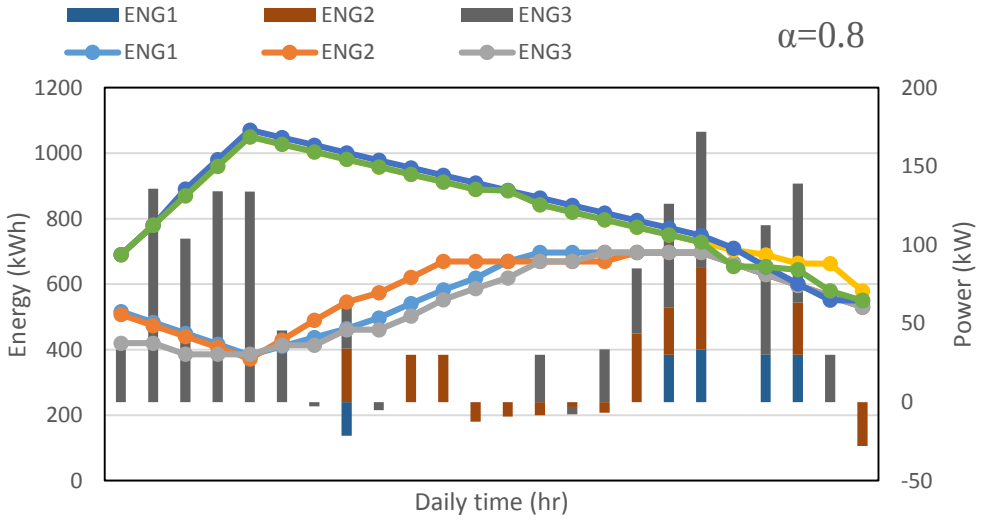
ENG1
ENG2
ENG3
ENG1
ENG2
ENG3
α=0.8
Energy (kWh)
Power (kW)
Daily time (hr)
0
200
400
600
800
1000
1200
-50
0
50
100
150
200

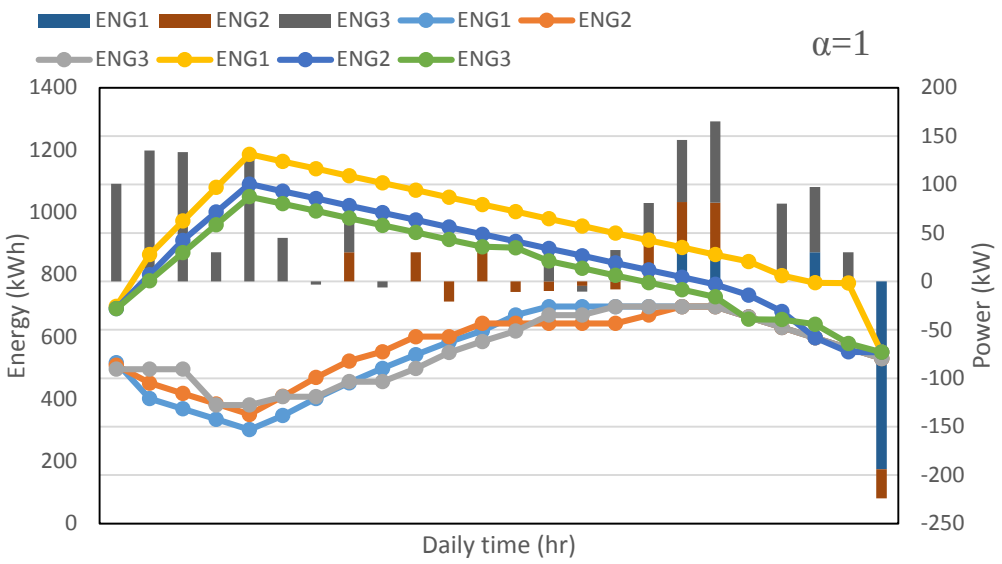

Fig. 6. Daily energy management in case 1: energy available at BESs and EVs parking, and power trading between ENGs and upstream network.

Table 6 shows how different levels of maximum electric vehicle discharge power ($P_{dis,ev}^{max}$) influences the generation mix and costs. As it can be seen, the increase and decrease in this parameter might not change the type of ENGs and the three buildings are all AC nanogrids. This is predictable because changes in this parameter have similar and common effect in both DC and AC investment cost and power balance equations. On the other hand, changes in this parameter do not have a significant impact on the mix of ENGs' generation systems, corresponding installation capacity, and the capacity of the BES. Consequently, investment and maintenance costs would not have meaningful variation.

As expected, since electric vehicles should contribute to supply customer demand during peak load hours and should be charged in the morning early a day, the variation in the maximum discharge power of electric vehicles can only affect the hourly power generation pattern and the operating cost of DERs. At ENG1, once $P_{dis,ev}^{max}$ is not more than 50 kW, the operation cost is low because there is not power enough in EVs park lot, so no need to charge them and buy electricity much from the upstream network. As a result, surplus electricity from the storage system can be sold.

By increasing $P_{dis,ev}^{max}$ to 100 kW, it reduces power sales and increases energy purchasing as EVs' charging increases. At higher values of this parameter, although the amount of charging power of EVs rises, EVs at peak load can assist generation systems in providing energy for customers, decreases power purchase, and rises the sale. As a result, the operating cost is reduced again. The bar chart in Fig. 8 supports this idea; when $P_{dis,ev}^{max} = 100$ kW, purchasing electrical energy is considerably high, whereas for other amounts of this parameter, selling energy would overcome receiving it from the main grid.

Another noticeable point is the operation cost at ENG2. When $P_{dis,ev}^{max} = 150$ kW, the capacity of the solar system has also increased slightly. So, the pattern of power generation and distribution at the building has changed.

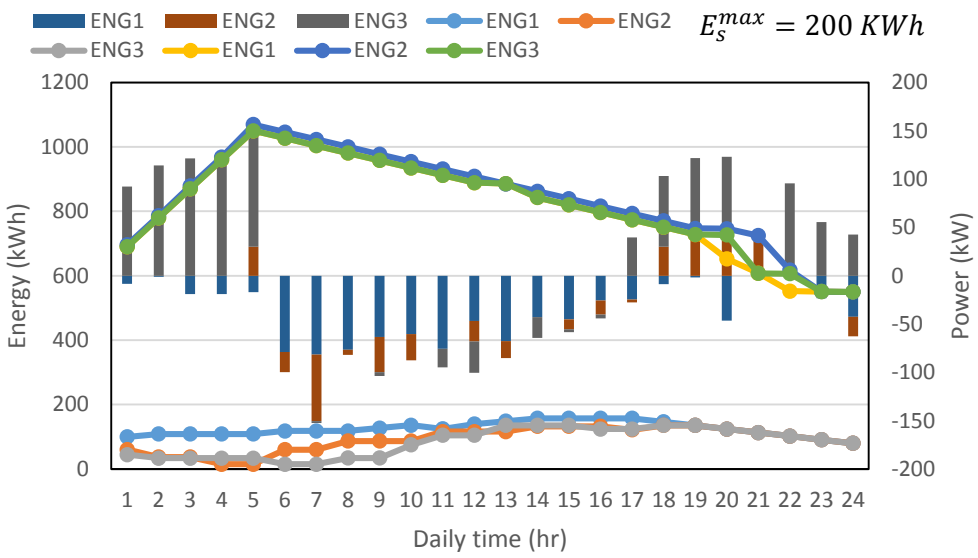
ENG1
ENG2
ENG3
ENG1
ENG2
ENG3
ENG1
ENG2
ENG3
$E_s^{max} = 200\ KWh$
Energy (kWh)
Power (kW)
Daily time (hr)

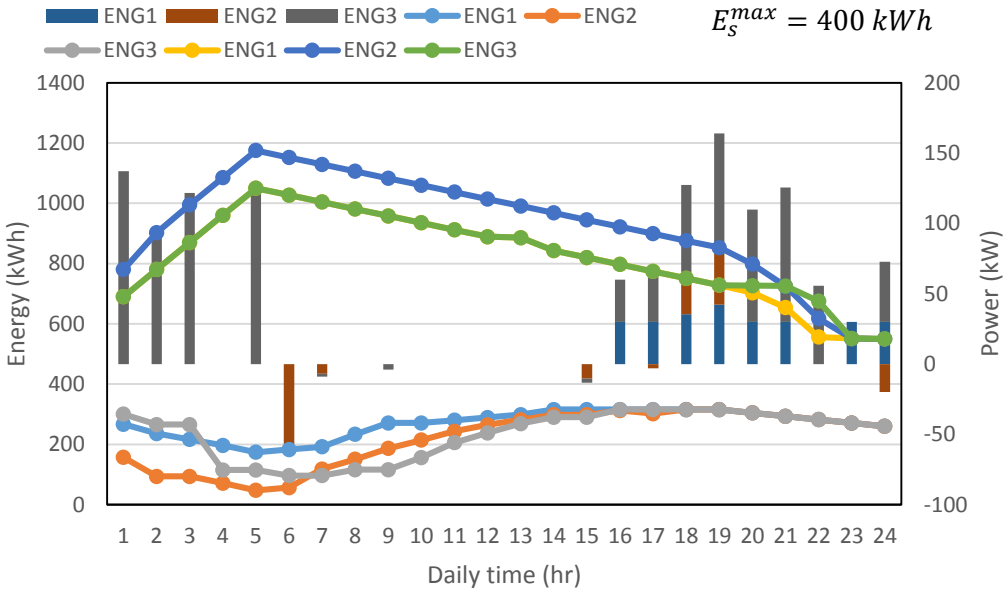
ENG1
ENG2
ENG3
ENG1
ENG2
ENG3
ENG1
ENG2
ENG3
$E_s^{max} = 400\ kWh$
Energy (kWh)
Power (kW)
Daily time (hr)

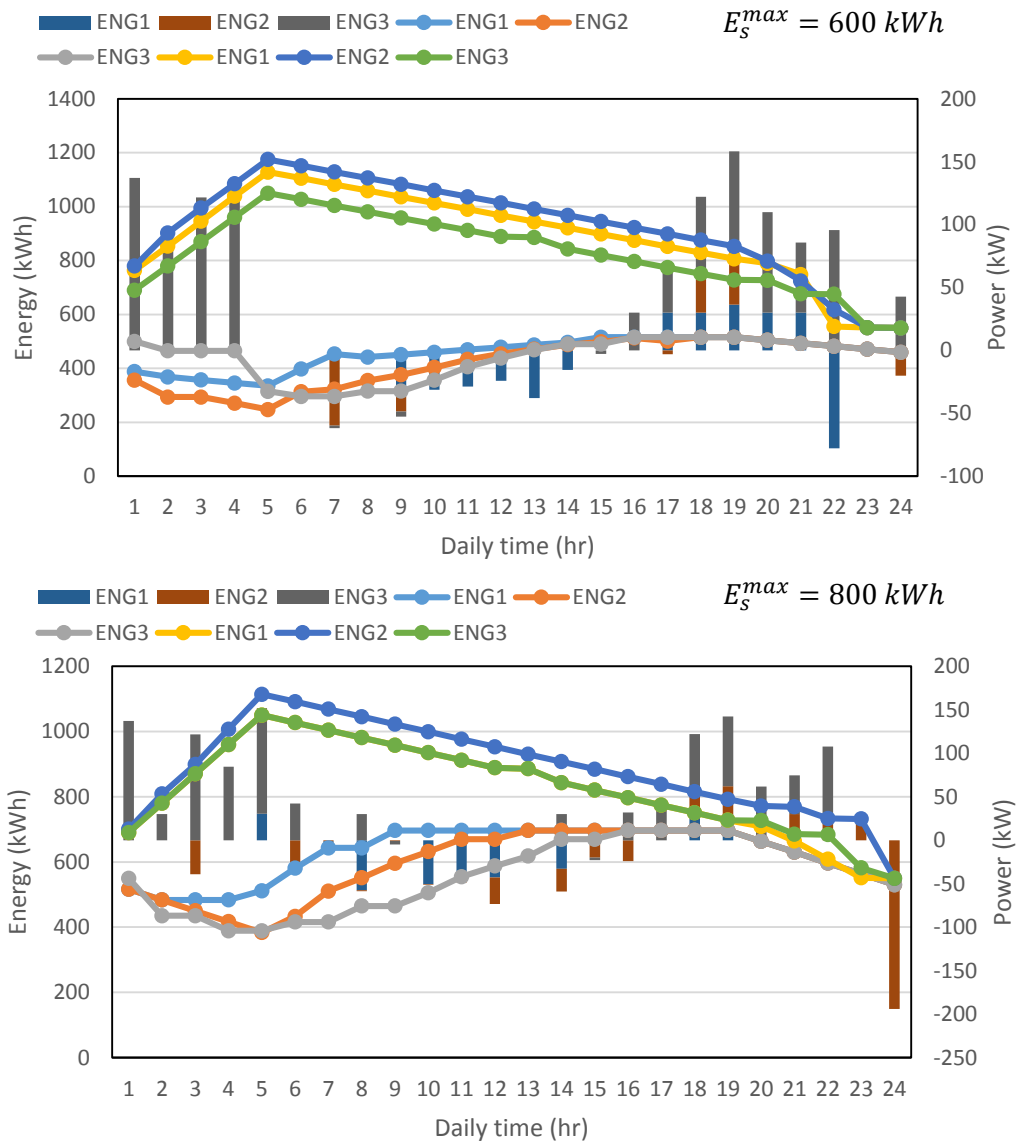

Fig. 7. Daily energy management in case 2: energy available at BESs and EVs parking, and power trading between ENGs and upstream network.

In this case, electric vehicles at ENG2 assist solar energy systems at peak time, and as the capacity of the solar system increases, there is no need to purchase electricity from the grid to charge electric vehicles at the early hours of a day. These reasons have led to a negative operation cost at this ENG. Looking at both Table 4 and bar chart in Fig. 8, it is interesting that, although the increase in $P_{dis,ev}^{max}$ at ENG3 may affect delivering and receiving electrical energy to/from the main grid, the operation cost of this active building does not vary in total. This implies that EV park lot has a neutral influence on the operation, generation mix, and the type of active building at ENG3.

The line graph in Fig. 8 shows that for all amount of $P_{dis,ev}^{max}$, BES system at three active buildings have to deliver electrical energy at early hours to help charge EVs' battery to be prepared for leaving the lot, with the exception of $P_{dis,ev}^{max} = 50$ kW and $P_{dis,ev}^{max} = 150$ kW at ENG1 where energy storage at BES is stable. It is expected that, an increase in $P_{dis,ev}^{max}$ supports the generation system to supply the demand power, making EVs discharge their energy. This pattern definitely results in more charging at ENGs by purchasing from the main grid, DERs generation, and BES system. However, because the load demand at ENG1 and ENG3 at early hours of the day is more than that of ENG2, energy at park lot at ENG1 and ENG3 dips first, then rises as ENG2.

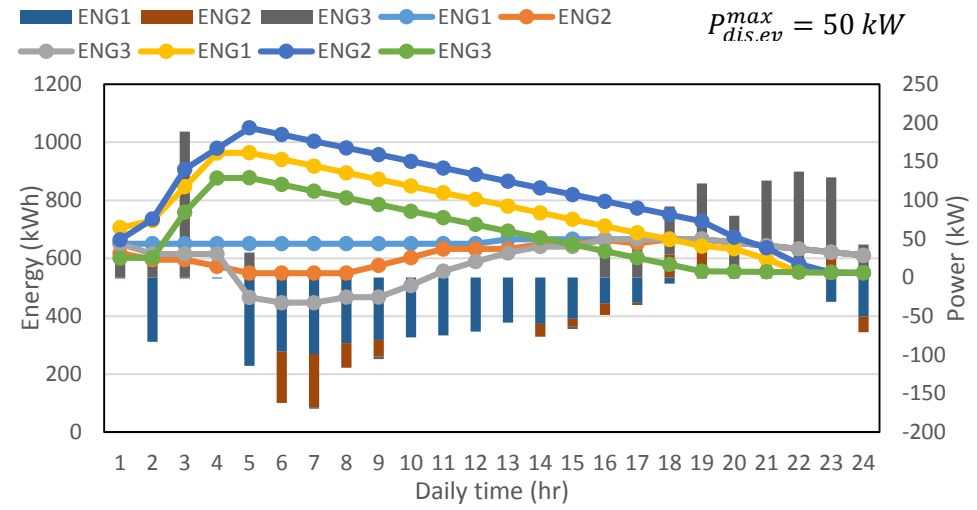
ENG1 ENG2 ENG3 ENG1 ENG2 ENG3 ENG1 ENG2 ENG3
$P_{dis,ev}^{max} = 50\ kW$
Energy (kWh)
Power (kW)
Daily time (hr)

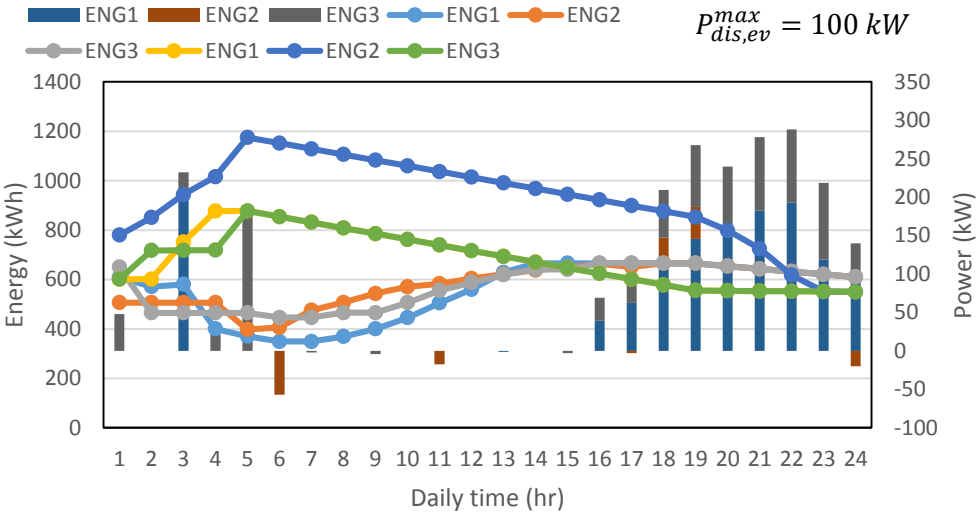
ENG1 ENG2 ENG3 ENG1 ENG2 ENG3 ENG1 ENG2 ENG3
$P_{dis,ev}^{max} = 100\ kW$
Energy (kWh)
Power (kW)
Daily time (hr)

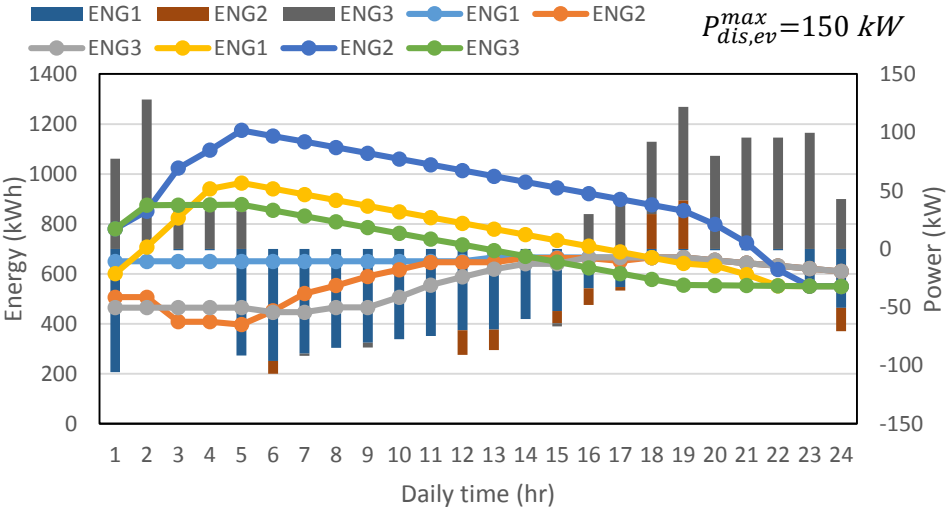
ENG1 ENG2 ENG3 ENG1 ENG2 ENG3 ENG1 ENG2 ENG3
$P_{dis,ev}^{max}$=150 kW
Energy (kWh)
Power (kW)
Daily time (hr)

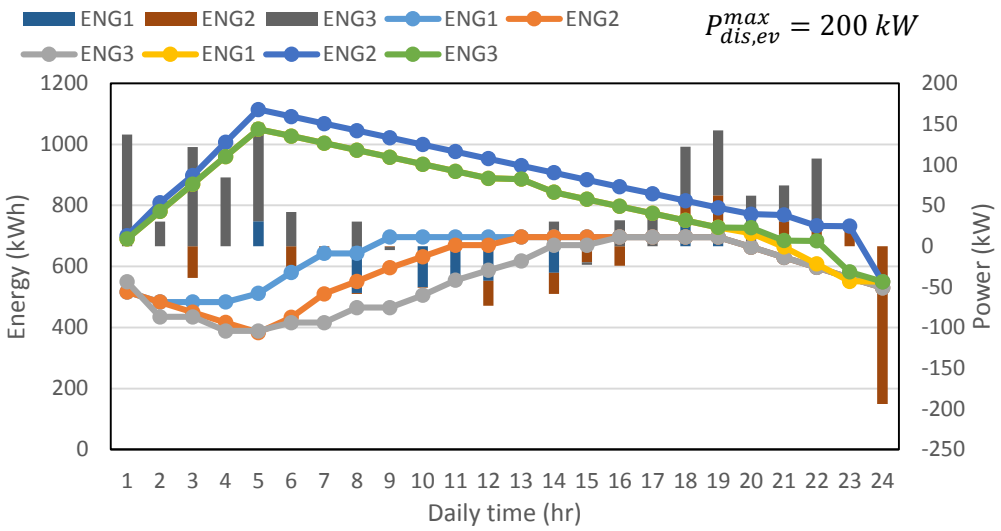

Fig. 8. Daily energy management in case 3: energy available at BESs and EVs parking, and power trading between ENGs and upstream network.

5. CONCLUSION

This paper has presented a planning framework for active buildings as an Energy Nano-Grid with the goals of determining the optimal size and the generation mix of the distributed energy resources and battery energy storage system, the ENG type (AC or DC), as well as the optimal daily load sharing as an energy management (EM) system. To implement a deep assessment, three factors have been considered: ratio of DC load, maximum allowable installation capacity of BES, and upper bound of EVs' discharge power availability, for various case studies and a MILP solver has been adopted. According to the simulation results, the type of ENGs would be DC when the rate of the DC load increases, through reducing investment and operation costs. The stability of demand and capacity constraints meant that this parameter did not have a major influence on the generation mix, the capacity of DERs and BESs and the energy of EVs in the park lots. In contrast to the DC load percentage, the maximum capacity limit for the BES system can directly change the capacity of the DERs and the investment and operating costs, as it plays an important role, sometimes as a supply resource and sometimes as a load. So, it might modify the pattern of generation and consumption. Due to not having a significant role at ENGs during the whole day, different level of EVs' maximum discharge power does not make any meaningful changes in the generation mix and in the investment cost. However, it could only change the power supply at peak hours. So, operation cost and discharge power of EVs parking are the only factors that vary noticeably. Because of increase in various gadgets and dc loads in the user side such as computer, TV, refrigerator and so on, working in different voltage levels and consumption pattern, it would be meaningful to analysis these types of load individually, and be significant to evaluate how they separately affect the other variables and planning results. These points may be the future study perspective of the authors.

REFERENCES

[1] World Energy Council in partnership with OLIVER WYMAN. (2018) World energy trilemma index 2018. [Online]. Available: https://www.worldenergy.org/wp-content/uploads/2018/ 10/World-Energy-Trilemma-Index-2018.pdf

[2] The Active Building Centre (ABC). (2018) EPSRC. [Online]. Available: https://www.activebuildingcentre.com/

[3] S. Senemar, A. Seifi, and M. Rastegar, Optimal Operation of Renewable- Based Residential Energy Hubs for Minimizing PV Curtailment. Cham: Springer International Publishing, 2018, pp. 271–295. [Online]. Available: https://doi.org/10.1007/978-3-319-75097-2 12

[4] S. Bracco, F. Delfino, G. Piazza, F. Foiadelli, and M. Longo, "Nanogrids with renewable sources, electrical storage and vehicle-to-home systems in the household sector: Analysis for a single-family dwelling," in 2019 IEEE Milan PowerTech. IEEE, 2019, pp. 1–6.

[5] W. Tushar, T. K. Saha, C. Yuen, D. Smith, and H. V. Poor, "Peer-topeer trading in electricity networks: an overview," IEEE Transactions on Smart Grid, 2020.

[6] B. Nordman and K. Christensen, "Local power distribution with nanogrids," in 2013 International green computing conference proceedings. Ieee, 2013, pp. 1–8.

[7] M. Ban, M. Shahidehpour, J. Yu, and Z. Li, "A cyber-physical energy management system for optimal sizing and operation of networked nanogrids with battery swapping stations," IEEE Transactions on Sustainable Energy, vol. 10, no. 1, pp. 491–502, 2017.

[8] H. Lotfi and v. Khodaei, Amin, "Ac versus dc microgrid planning," IEEE Transactions on Smart Grid, vol. 8, no. 1, pp. 296–304, 2015.

[9] H. Lotfi and A. Khodaei, "Hybrid AC/DC microgrid planning," Energy, vol. 118, pp. 37–46, 2017.

[10] R. P. Chandrasena, F. Shahnia, A. Ghosh, and S. Rajakaruna, "Operation and control of a hybrid ac-dc nanogrid for future community houses," in 2014 Australasian Universities Power Engineering Conference (AUPEC). IEEE, 2014, pp. 1–6.

[11] S. Senemar, M. Rastegar, M. Dabbaghjamanesh, and N. D. Hatziargyriou, "Dynamic structural sizing of residential energy hubs," IEEE Transactions on Sustainable Energy, 2019.

[12] N. Liu, X. Yu, W. Fan, C. Hu, T. Rui, Q. Chen, and J. Zhang, "Online energy sharing for nanogrid clusters: A lyapunov optimization approach," IEEE Transactions on Smart Grid, vol. 9, no. 5, pp. 4624–4636, 2017.

[13] S. Teleke, L. Oehlerking, and M. Hong, "Nanogrids with energy storage for future electricity grids," in 2014 IEEE PES T&D Conference and Exposition. IEEE, 2014, pp. 1–5.

[14] M. Heidari, T. Niknam, M. Zare, and S. Niknam, "Integrated battery model in cost-effective operation and load management of grid-connected smart nano-grid," IET Renewable Power Generation, vol. 13, no. 7, pp. 1123–1131, 2019.

[15] M. R. Sandgani and S. Sirouspour, "Energy management in a network of grid-connected microgrids/nanogrids using compromise programming," IEEE Transactions on Smart Grid, vol. 9, no. 3, pp. 2180–2191, 2016.

[16] H. Farzin, M. Fotuhi-Firuzabad, and M. Moeini-Aghtaie, "A stochastic multi-objective framework for optimal scheduling of energy storage systems in microgrids," IEEE Transactions on Smart Grid, vol. 8, no. 1, pp. 117–127, 2016.

[17] N. B. Arias, A. Tabares, J. F. Franco, M. Lavorato, and R. Romero, "Robust joint expansion planning of electrical distribution systems and ev charging stations," IEEE Transactions on Sustainable Energy, vol. 9, no. 2, pp. 884–894, 2017.

[18] S. Sheng, P. Li, C.-T. Tsu, and B. Lehman, "Optimal power flow management in a photovoltaic nanogrid with batteries," in 2015 IEEE Energy Conversion Congress and Exposition (ECCE). IEEE, 2015, pp. 4222–4228.

[19] J. Kumar, A. Agarwal, N. Singh, "PV fed Hybrid Energy Storage System Supported DC Microgrid," in 2019 IEEE 1st International Conference on Energy, Systems and Information Processing (ICESIP), IEEE, 2019.

[20] J. Kumar, A. Agarwal, and N. Singh, ''Design, operation and control of a vast DC microgrid for integration of renewable energy sources,'' Renew. Energy Focus, vol. 34, pp. 17–36, Sep. 2020.

[21] Kumar J, Agarwal A, Singh N. Multipurpose water storage tank based DC microgrid system for isolated communities. Energy Storage. 2022; 4(4):e308. doi:10.1002/est2.308

[22] J. Kumar, A. Agarwal, and V. Agarwa, Optimized Design of Mini-grid System for Hilly Region, IETE Journal of Research, 2019. DOI: 10.1080/03772063.2019.1620642.

[23] A. Sangwongwanich, Y. Yang, and F. Blaabjerg, "High-performance constant power generation in grid-connected PV systems," IEEE Trans. Power Electron., vol. 31, no. 3, pp. 1822–1825, 2016.

[24] A. Sangwongwanich, Y. Yang, F. Blaabjerg, and H. Wang, "Benchmarking of constant power generation strategies for single-phase gridconnected photovoltaic systems," IEEE Trans. Ind Appl., vol. 54, no. 1, pp. 447–457, Jan./Feb. 2018.

[25] L. Qu and W. Qiao, "Constant power control of DFIG wind turbines with supercapacitor energy storage," IEEE Trans. Ind. Appl., vol. 47, no. 1, pp. 359–367, Jan./Feb. 2009.

[26] Solar home electricity data. (2014) Ausgrid. [Online]. Available: https://www.ausgrid.com.au/Industry/Our-Research/Data-to_share/ Solar-home-electricity-data

[27] Electric cars available in Australia. (2019) canstarblue. [Online]. Available: https://www.canstarblue.com.au/vehicles/ electric-cars-available-australia/

[28] Journey to work in Australia. (2016) Abs beta. [Online]. Available: https://www.abs.gov.au/ausstats/abs@.nsf/Lookup/by

[29] Distributed Generation Renewable Energy Estimate of Costs. (2019) Transforming energy. [Online]. Available: https://www.nrel.gov/analysis/ tech lcoe re cost est.html,

[30] S. Schoenung, "Energy storage systems cost update," SAND2011-2730, vol. 606, 2011.

[31] List of Converters Prices. (2019) Alibaba. [Online]. Available: https://www.alibaba.com/trade/search?fsb=y&IndexArea=product en&CatId=&SearchText=converters

[32] Converters. (2019) Amazon. [Online]. Available: https://www.amazon. com/s?k=converter&ref=nb sb noss